Biochemical and Biophysical Research Communications 386 (2009) 111–117

Contents lists available at ScienceDirect

Biochemical and Biophysical Research Communications

journal homepage: www.elsevier.com/locate/ybbrc

hERG1a/1b heteromeric currents exhibit amplified attenuation of inactivation in variant 1 short QT syndrome

M.J. McPate [a,1], H. Zhang [b], J.M. Cordeiro [c], C.E. Dempsey [d], H.J. Witchel [a,2], J.C. Hancox [a,*]

[a] Department of Physiology and Pharmacology, Bristol Heart Institute, School of Medical Sciences, The University of Bristol, University Walk, Bristol BS8 1TD, UK
[b] Biological Physics Group, School of Physics and Astronomy, The University of Manchester, Manchester M13 9PL, UK
[c] Masonic Medical Research Laboratory, 2150 Bleecker St., Utica, NY 13501-1787, USA
[d] Department of Biochemistry, School of Medical Sciences, The University of Bristol, University Walk, Bristol BS8 1TD, UK

ARTICLE INFO

Article history:
Received 26 May 2009
Available online 6 June 2009

Keywords:
Channelopathy
hERG
hERG1a/1b
hERG1b
QT interval
Rapid delayed rectifier
Short QT syndrome

ABSTRACT

Potassium channels encoded by *hERG* (human ether-à-go-go-related gene) underlie the cardiac rapid delayed rectifier K^+ current (I_{Kr}) and *hERG* mutations underpin clinically important repolarization disorders. Virtually all electrophysiological investigations of hERG mutations have studied exclusively the hERG1a isoform; however, recent evidence indicates that native I_{Kr} channels may be comprised of hERG1a together with the hERG1b variant, which has a shorter N-terminus. Here, for the first time, electrophysiological effects were studied of a gain-of-function hERG mutation (N588K; responsible for the 'SQT1' variant of the short QT syndrome) on current ($I_{hERG1a/1b}$) carried by co-expressed hERG1a/1b channels. There were no significant effects of N588K on $I_{hERG1a/1b}$ activation or deactivation, but N588K $I_{hERG1a/1b}$ showed little inactivation up to highly positive voltages ($\leqslant$+80 mV), a more marked effect than seen for hERG1a expressed alone. $I_{hERG1a/1b}$ under action potential voltage-clamp, and the effects on this of the N588K mutation, also showed differences from those previously reported for hERG1a. The amplified attenuation of I_{hERG} inactivation for the N588K mutation reported here indicates that the study of co-expressed hERG1a/1b channels should be considered when investigating clinically relevant hERG channel mutations, even if these reside outside of the N-terminus region.

Introduction

In recent years a novel cardiac repolarization disorder called the short QT syndrome (SQTS) has been identified that is characterized by marked abbreviation of the QT interval on the electrocardiogram, changes in T wave morphology, poor rate adaptation of the QT interval and an increased risk of arrhythmia and sudden death [1–4]. Gain-of-function mutations in three potassium (K^+) channel genes have been identified in SQTS patients: the SQT1 variant of the syndrome is linked to mutations to *KCNH2*, whilst SQT2 and SQT3 variants are associated, respectively, with mutations to *KCNQ1* and *KCNJ2* [5–7]. With a strong correlation between the SQTS and increased arrhythmia susceptibility [4,8], this syndrome provides an important opportunity to understand the link between accelerated cardiac repolarization and arrhythmogenesis; indeed, the SQTS has been proposed to provide a paradigm for understanding the role of cardiac K^+ channels in ventricular fibrillation [9].

The first cardiac K^+ current implicated in the SQTS was the rapid delayed rectifier (I_{Kr}), the channel α subunit of which is encoded by *KCNH2* (alternative nomenclature *hERG*: *human ether-à-go-go-related gene*) [5,6]. I_{Kr} plays a critical role in ventricular action potential (AP) repolarization and, thereby, in determining the duration of the QT interval [10]. SQT1 patients were found to possess an asparagine to lysine substitution (N588K) in the S5-Pore linker region of the hERG channel protein [5,6], resulting in attenuation of a rapid C-type inactivation process that normally limits hERG current (I_{hERG}) amplitude at positive voltages [11,12]. In turn, this is envisaged to enable greater repolarizing current to flow through SQT1 mutant than wild-type (WT) channels during cardiac APs [5,11–13].

Although studies conducted to-date have provided insight into the possible basis of abbreviated repolarization in SQT1 [5,11–13], there is some question as to their physiological relevance. This is because – in common with virtually all studies of recombinant hERG channels that have been conducted to-date – *all* information on the likely consequences for I_{Kr} kinetics of the N588K hERG mutation comes from studies of the hERG1a isoform [5,11–14]. Recent evidence, however, suggests that native cardiac I_{Kr} may not be

* Corresponding author.
E-mail address: jules.hancox@bristol.ac.uk (J.C. Hancox).
[1] Present address: Novartis Institutes for Biomedical Research, Horsham, West Sussex RH12 5AB, UK.
[2] Present address: Medical Research Building, Brighton and Sussex Medical School, Falmer BN1 9PX, UK.

0006-291X/$ - see front matter © 2009 Elsevier Inc. All rights reserved.
doi:10.1016/j.bbrc.2009.05.134

comprised of hERG1a alone, but rather of hERG1a heteromerically expressed with an alternative transcript, hERG1b, an isoform with a truncated N-terminus [15,16]. The ERG1b splice variant was initially identified in both mouse and human hearts and is identical to the 1a isoform except for a truncated N-terminus [17,18]. It was subsequently proposed not to be expressed at the protein level in human heart [19]; however, the ERG1a and 1b isoforms have now been found to co-exist in several species and are co-localized in the T-tubules of ventricular myocytes [15]. They co-assemble to form functional heteromeric channels with altered kinetics (particularly in respect of deactivation) that may more closely recapitulate native I_{Kr} compared to ERG1a alone [15,16]. Very recent evidence of altered WT hERG channel gating for co-expressed hERG1a/1b [16,20] raises questions as to whether or not consequences for native I_{Kr} of disease-causing hERG mutations, including those that affect I_{hERG} inactivation, can be considered to be adequately recapitulated by studying hERG1a alone. Consequently, the present study was conducted to determine the effects of the N588K hERG SQT1 mutation on co-expressed hERG1a/1b channels. This report shows for the first time that, despite the fact that the location of the S5-Pore linker in the hERG channel is distant from that of the N-terminus, the effects of the SQT1 N588K hERG mutation on I_{hERG} carried by hERG1a/1b channels are more marked than those reported previously for hERG1a alone.

Methods

Maintenance of hERG expressing cell lines. WT hERG1b in pcDNA 3.1 was generously donated by Dr. Gail Robertson (University of Wisconsin). The construction of N588K hERG1a from WT hERG in pcDNA 3.0 vector has been described previously [12]. N588K hERG1b was made by replacement of the N-terminus in N588K 1a with that of WT hERG1b. This was achieved by 2-primer PCR of hERG1b (in pcDNA3.1) with the creation of a SalI restriction site (located in the S2 domain of hERG). The resulting PCR product was cut at SalI and HindIII sites and sub-cloned into the hERG1a vector (in pcDNA3.0). Chinese Hamster Ovary (CHO) cells were passaged using a non-enzymatic agent (Splitase, AutogenBioclear) and plated out onto small sterilised glass coverslips in 30 mm petri dishes containing Kaighn's modification of Ham's F12-K medium (Gibco), supplemented with 10% foetal bovine serum (Gibco) and 200 $\mu g\,ml^{-1}$ gentamicin (Gibco). Prior to transfection, cells were plated out onto small sterilised glass coverslips. After 24 h cells were co-transfected with hERG and green fluorescent protein (in pCMX; donated by Dr. Jeremy Tavare) at a ratio of 2:1 using Lipofectamine LTX (Invitrogen), according to the manufacturer's instructions. For the experiments performed using hERG1a and 1b co-expression, the cells were co-transfected with WT or N588K hERG1a and 1b at a co-expression ratio of 1:1. Following transfection, after 5–6 h incubation in serum-containing medium, medium was replaced. Cells were incubated at 37 °C for at least 1 day prior to electrophysiological study. Data from WT and N588K hERG1a expressed alone (Fig. 3) derive from CHO cells stably expressing WT or N588K hERG1a [12,21].

Electrophysiological recording. Data acquisition and recording methods used were identical to those described in previous studies of WT and N588K hERG1a from our laboratory [12,13,22]. Briefly, whole-cell voltage-clamp measurements were made at 37 °C with an external solution containing (in mM): 140 NaCl, 4 KCl, 2.5 $CaCl_2$, 1 $MgCl_2$, 10 Glucose and 5 HEPES (titrated to pH 7.45 with NaOH). The pipette dialysis solution contained (in mM): 130 KCl, 1 $MgCl_2$, 5 EGTA, 5 MgATP and 10 HEPES (titrated to pH 7.2 with KOH). Pipette resistance ranged from 1.5–3.5 MΩ. Typically ~80% series resistance could be compensated. The action potential (AP) waveforms used for 'AP clamp' experiments (Fig. 4) are identical to those described in [13].

Data analysis and presentation. The numerical equation for voltage-dependence of activation is described in [12]. The use of a conventional 'availability' voltage-protocol to quantify the voltage-dependence of I_{hERG} inactivation (e.g. [11,12]) is contingent upon the ability to inactivate fully I_{hERG} with strong membrane depolarization. However, in this study N588K $I_{hERG1a/1b}$ could not be substantially inactivated by depolarizations as positive as +80 mV (Fig. 3) and so we adopted an approach to quantify inactivation similar to that used in a recent investigation of inactivation-attenuating hERG mutations [22]. For each of several test voltages (+20, +40, +60, +80 mV; Fig. 3) a 2 s depolarization (to activate/inactivate I_{hERG}) was followed by a brief (2 ms) hyperpolarization to −100 mV (to relieve inactivation) and then inactivation was re-established by a 2 s depolarization to the same potential as the first step. The magnitude of the current transient during the third step of the protocol indicated I_{hERG} at each voltage after pronounced recovery from inactivation, whilst the sustained current at the end of the first pulse was taken as representing current remaining after inactivation was complete at the relevant test voltage. The ratio of the two was used to assess the fraction of inactivated I_{hERG} at each test voltage.

Data were analysed using Clampfit 8 (Axon Instruments), Excel 2002 and Prism v3 (Graphpad Inc.) software. Throughout, data are presented as the mean ± standard error of the mean (SEM). Statistical analysis was carried out using a Student's *t*-test and one or two-way analysis of variance (ANOVA) as appropriate, with Bonferroni post-test using Prism v3 (Graphpad Inc.). *P* values of less than 0.05 were taken to be statistically significant.

Results and discussion

Fig. 1A shows representative records of I_{hERG} elicited by a depolarizing voltage command to +20 mV from a holding potential of −80 mV (protocol shown as inset; [12,13,23]), for each of singly-expressed WT (Ai) and N588K (Aii) hERG1b channels. For both channels, I_{hERG1b} amplitude during the depolarizing voltage command was much greater than the subsequent I_{hERG1b} 'tail' visible on repolarization to −40 mV; tail current deactivation was also extremely rapid (with mono-exponential time-constants <30 ms for both WT and N588K hERG1b). The lack of a resurgent I_{hERG} tail and extremely rapid deactivation time-course for WT I_{hERG1b} indicates that, concordant with previous evidence [17,18], WT I_{hERG1b} expressed alone does not recapitulate native I_{Kr}; therefore all further experiments were conducted using co-expressed hERG1a/1b. Fig. 1B shows I_{hERG} families for each of WT (Bi) and N588K (Bii) $I_{hERG1a/1b}$ elicited by commands to a range of test voltages (Fig. 1B lower traces; cf. [12]). WT $I_{hERG1a/1b}$ increased progressively with depolarization up to ~−10 mV and then declined at more positive potentials, whereas N588K $I_{hERG1a/1b}$ increased progressively up to ~+40/+50 mV, declining only slightly at +60 mV. Fig. 1Ci illustrates this graphically for mean end-pulse current data. Resurgent $I_{hERG1a/1b}$ tails for WT hERG were evident, whilst for N588K $I_{hERG1a/1b}$ tails were markedly smaller than pulse currents following commands to positive voltages (Fig. 1Bii). Normalized peak $I_{hERG1a/1b}$ tail – voltage relations were plotted (Fig. 1Cii) to ascertain parameters describing voltage-dependent activation for the two channels (cf. [12]). The calculated half-maximal activation voltage ($V_{0.5}$) values for WT and N588K $I_{hERG1a/1b}$ were, respectively, −27.0 ± 0.4 mV and −27.3 ± 1.1 mV, with corresponding *k* values of 7.4 ± 0.4 and 8.0 ± 1.0 mV ($n = 8$ cells each; $P > 0.05$ for both). These values are significantly more negative ($P < 0.001$) than those we have previously reported for WT and N588K I_{hERG1a} alone, under identical recording conditions (−20.1 ± 0.1 and −22.4 ± 0.6 mV, respectively,

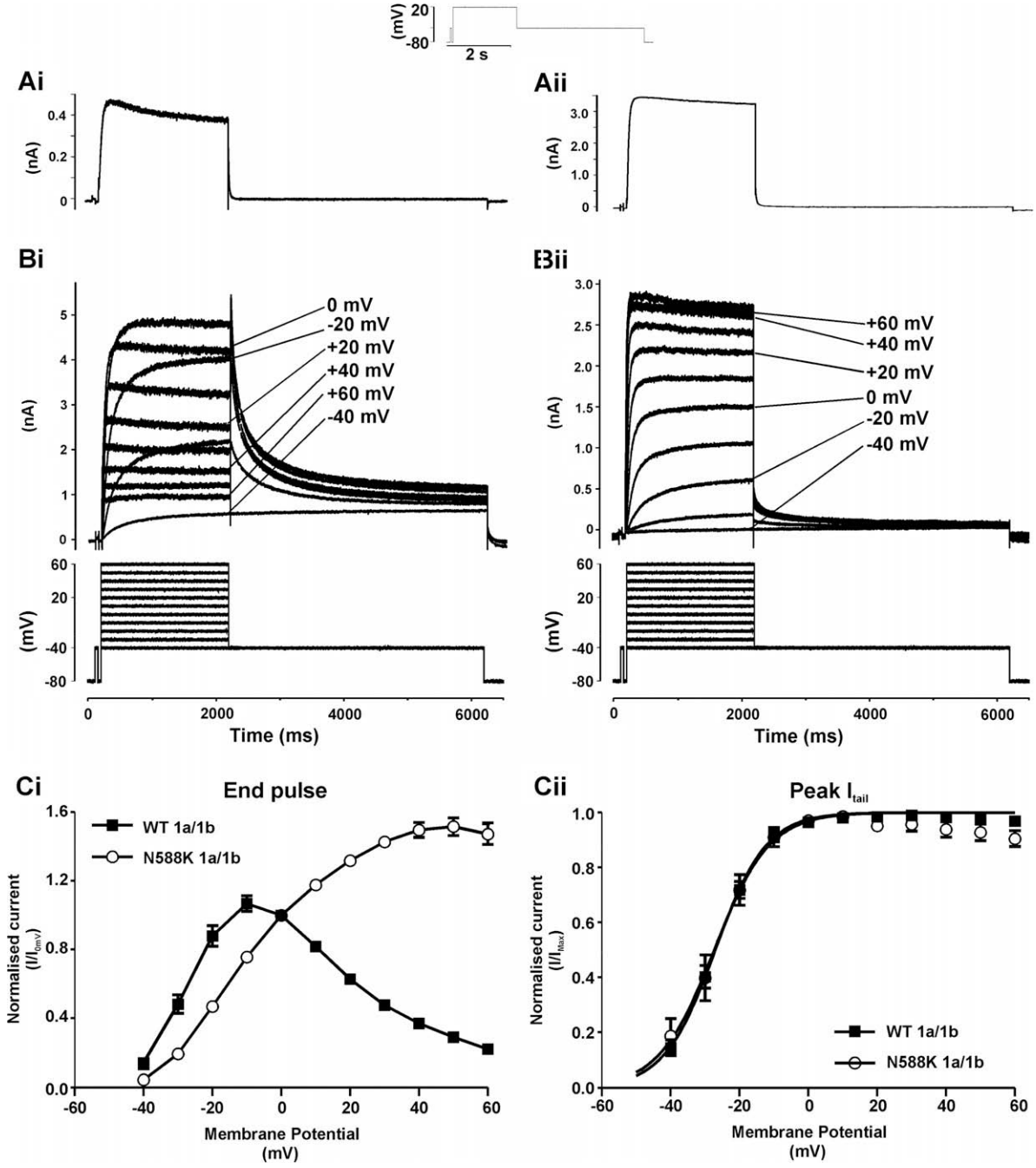

Fig. 1. *I–V* relations for WT and N588K $I_{hERG1a/1b}$. (A) Traces of WT (Ai) and N588K (Aii) I_{hERG1b} elicited by protocol shown in panel inset. (B) Traces of WT (Bi) and N588K (Bii) $I_{hERG1a/1b}$ elicited by 2 s depolarizations ranging from −40 to + 60 mV, from a holding potential of −80 mV. The repolarization step to −40 mV produced the resultant outward I_{tail}. (C) Ci End-pulse currents normalised to the current observed at 0 mV and then plotted against membrane potential. Cii Plots of the peak I_{tails} on repolarization to −40 mV against membrane potential for WT and N588K hERG1a/1b. For Cii data for each cell were normalised to the maximal I_{tail} recorded; mean data were fitted with a Boltzmann equation to give $V_{0.5}$ values of −27.0 ± 0.4 and −27.3 ± 1.1 mV for WT 1a/1b and N588K 1a/1b-hERG, respectively, with respective *k* values of 7.4 ± 0.4 and 8.0 ± 1.0 mV (n = 8 for each).

[12] and cf. [20]). Collectively, the data in Fig. 1 indicate that, at 37 °C, the N588K mutation alters rectification of $I_{hERG1a/1b}$, but without significantly altering the voltage-dependence of activation (cf. [12]).

In order to compare I_{hERG} deactivation between WT and N588K $I_{hERG1a/1b}$ the protocol shown above Fig. 2A (inset) was used [12] and the decline of $I_{hERG1a/1b}$ tails at different repolarization voltages was compared using bi-exponential tail current fitting. There was no significant difference between WT and mutant $I_{hERG1a/1b}$ in either fast (Fig. 2Bi) or slow (Fig. 2Bii) time-constants of deactivation, nor in the relative contributions of the fast/slow deactivating components (Fig. 2Biii; n = 7 cells each). The deactivation time-course for WT and N588K $I_{hERG1a/1b}$ was, however, faster than that of the corresponding hERG1a channels (data not shown), consistent with accelerated deactivation reported previously for WT hERG1a/1b [16,18,20]. A plot of the fully-activated current–voltage (*I–V*) relation derived from this protocol (Fig. 2C; cf. [12,24]) confirmed impaired rectification of N588K $I_{hERG1a/1b}$ compared to WT $I_{hERG1a/1b}$, accompanied by a modest positive-shift in reversal potential (from −85.2 ± 0.4 mV to −78.7 ± 1.9 mV; n = 7

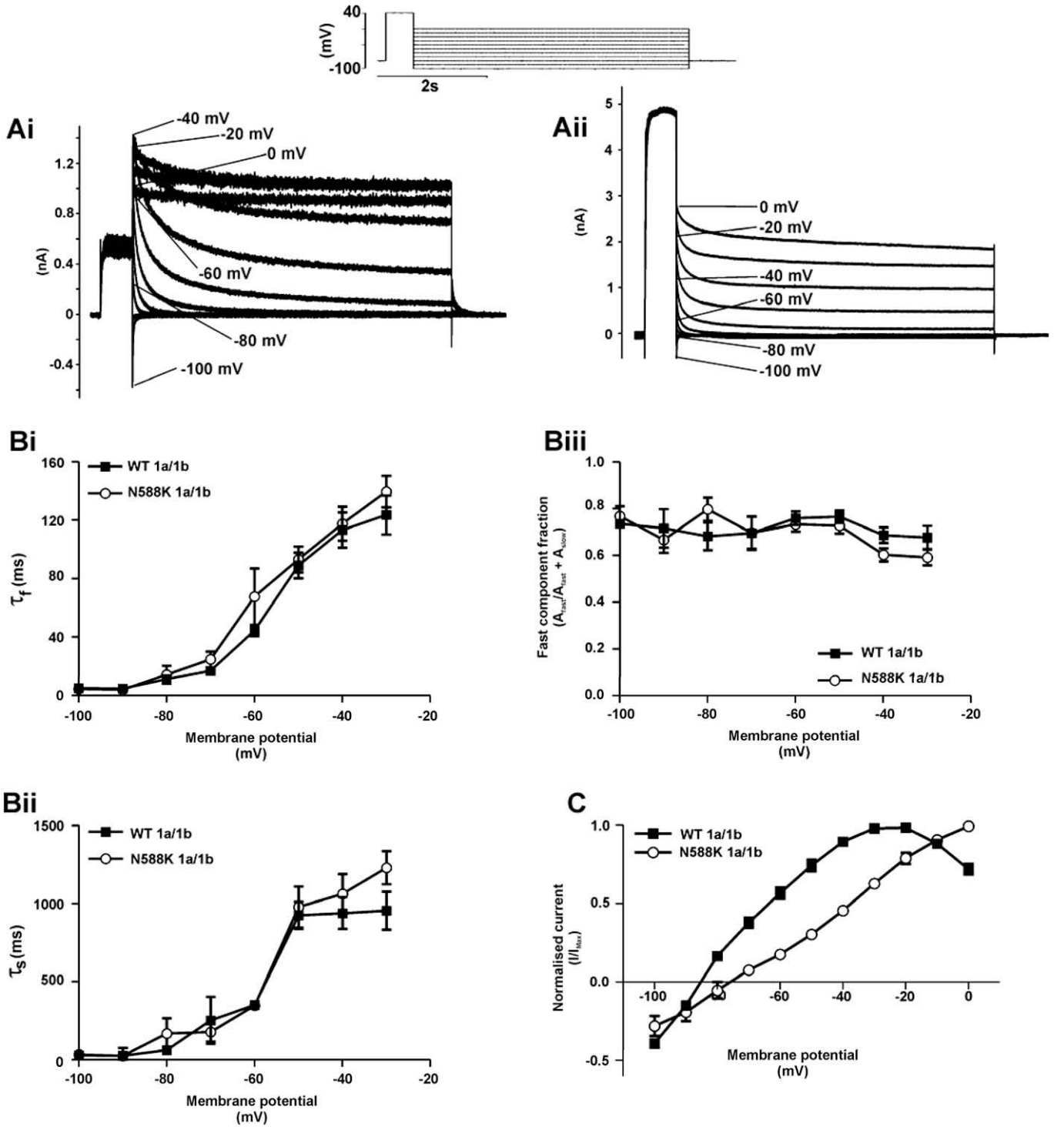

Fig. 2. Deactivation and the fully activated *I–V* relation. (A) Representative traces of WT (Ai) and N588K (Aii) $I_{hERG1a/1b}$ elicited by the protocol shown in the inset. (B) Plots of the fast (Bi) and slow (Bii) time-constants of deactivation for WT and N588K hERG1a/1b against membrane potential ($n = 7$, for each). Biii shows proportion of deactivation that can be attributed to the fast component for WT and N588K hERG1a/1b ($n = 7$). (C) The peak I_{tail} for WT and N588K hERG1a/1b plotted against the respective membrane potential and normalised to the peak outward I_{tail} observed for each individual cell ($n = 7$).

cells each) and relative pNa/pK ratio (from 0.0097 (WT) to 0.0201 (N588K)). These effects of the N588K hERG mutation are similar to those reported previously for hERG1a alone [12].

Recent evidence suggests inactivation gating of WT $I_{hERG1a/1b}$ is altered compared to that of WT I_{hERG1a} [16]. Given this, and also that the major reported effect of the N588K mutation on I_{hERG1a} is on the voltage-dependence of inactivation [11,12], it was imperative to determine effects of the N588K mutation on $I_{hERG1a/1b}$. The three-step protocol shown as an inset of Fig. 3A and B (see 'Methods' and [22]) was used to assess fractional inactivation of $I_{hERG1a/1b}$. As shown in Fig. 3A, at each of the 4 positive membrane potentials examined, WT $I_{hERG1a/1b}$ was substantially inactivated. By contrast, however, N588K $I_{hERG1a/1b}$ exhibited only a small transient component at any voltage, with a large sustained component

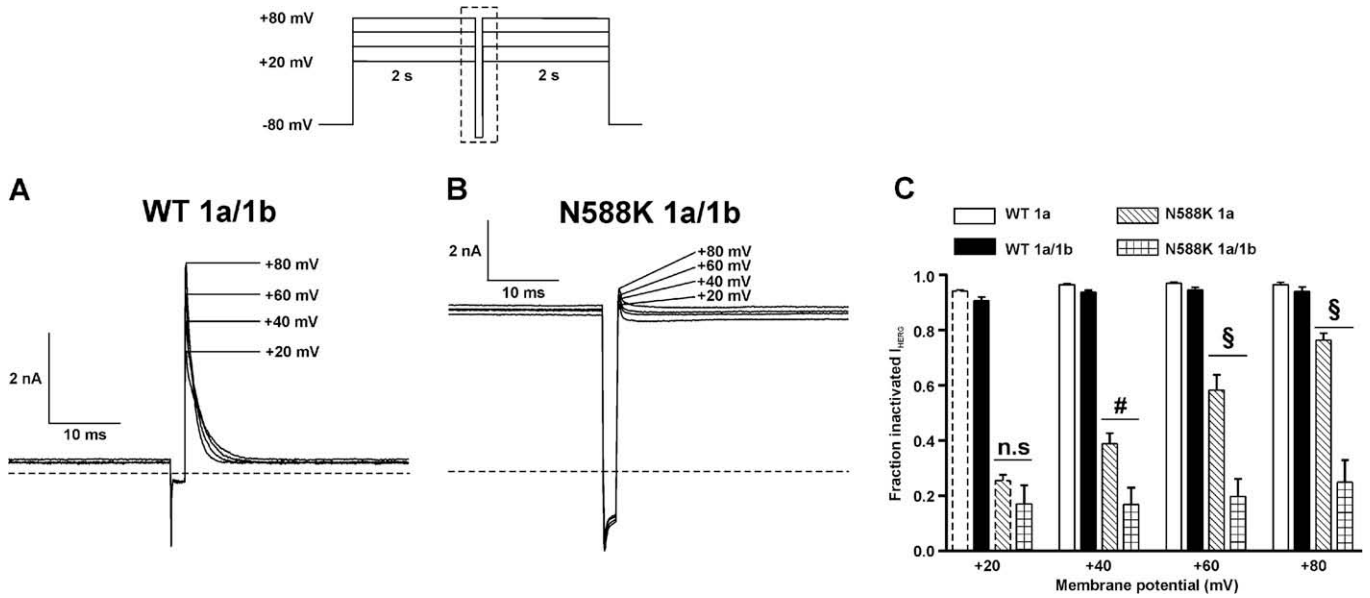

Fig. 3. I_{hERG} fractional inactivation. Representative current traces for WT (A) and N588K hERG1a/1b (B) that were elicited using the protocol shown in the inset (protocol not drawn to scale). The traces focus on the current profile during the second and third steps of the protocol, the area is indicated by the dashed box area in the protocol. The horizontal dashed line represents zero current. (C) The fraction of inactivated I_{hERG} at different membrane potentials shown for WT 1a (n = 5 cells), WT 1a/1b (n = 5 cells), N588K 1a (n = 5 cells) and N588K hERG1a/1b (n = 6 cells). n.s denotes no statistical significance, # denotes statistical significance of P < 0.01 and § denotes statistical significance of P < 0.001. Mean ± SEM values for WT 1a and N588K 1a at +20 mV highlighted by dashed bars are identical to those in [22].

(Fig. 3B), indicative of comparatively little fractional inactivation at any of the voltages examined. Fig. 3C shows mean data for WT and N588K $I_{hERG1a/1b}$, with mean data for WT and N588K I_{hERG1a} also included for comparison. There was little difference between WT I_{hERG1a} and $I_{hERG1a/1b}$ in fractional current inactivation at any voltage, whilst by contrast there was a very substantial difference at each voltage between N588K I_{hERG1a} and $I_{hERG1a/1b}$. Therefore, our data show that the inactivation-attenuating effects of the N588K mutation were markedly greater when co-expressed hERG1a and 1b were studied than when hERG1a alone was studied.

In order to assess the physiological consequences of the N588K mutation for co-expressed hERG1a and 1b, AP clamp experiments were performed. Fig. 4A shows representative currents for WT (Fig. 4Ai) and N588K (Fig. 4Aii) $I_{hERG1a/1b}$, elicited by a human ventricular AP command [13]. For WT $I_{hERG1a/1b}$ there was little current immediately following the AP upstroke, with current developing progressively throughout the AP plateau, declining during the terminal repolarization phase. Mean data from 14 cells showed that maximal WT $I_{hERG1a/1b}$ during AP repolarization occurred at −22.3 ± 1.0 mV. This value is significantly more positive than that we have recently reported for WT I_{hERG1a} during an identical AP command (−37.6 ± 1.7 mV; [13]) and the earlier peak $I_{hERG1a/1b}$ is consistent with faster deactivation together with accelerated activation and recovery from inactivation of $I_{hERG1a/1b}$ recently reported [16]. For N588K $I_{hERG1a/1b}$, current increased rapidly following the AP upstroke and peaked early during the AP plateau. Current then declined, with a relatively rapid decline during the final AP repolarization phase. Peak N588K $I_{hERG1a/1b}$ occurred at +27.1 ± 0.2 mV (n = 14), which compares with a value of +24.6 ± 0.6 mV for I_{hERG1a} during the same waveform [13] (P < 0.001). Current density plots for peak repolarizing $I_{hERG1a/1b}$ (Fig. 4C) show a markedly greater maximal repolarizing current for N588K than for WT $I_{hERG1a/1b}$ during a ventricular AP command waveform (P < 0.001).

For hERG1a, a differential effect of the N588K mutation on current during ventricular and Purkinje fibre APs has been suggested to contribute toward U wave formation and a pro-arrhythmic substrate in SQT1 [11,12]. Therefore, AP clamp experiments with a Purkinje fibre (PF) AP command [12] were also performed (Fig. 4B). For both WT (Bi) and N588K (Bii) $I_{hERG1a/1b}$, current during the PF AP was bow-shaped, peaking at −17.4 ± 3.0 mV (n = 13) and −9.0 ± 0.3 mV (n = 14; P < 0.001), respectively, (this compares with −45.6 ± 1.6 and −14.8 ± 0.3 mV for WT and N588K I_{hERG1a} during the same PF waveform under identical conditions [12]). Fig. 4C shows that peak repolarization current densities for both WT and N588K conditions during the PF AP were significantly lower than those during the ventricular AP command, and that the N588K mutation produced only a small increase in maximal repolarizing $I_{hERG1a/1b}$ amplitude, that was not statistically significant (P > 0.05). Thus, effects of the N588K mutation on current during the PF AP were small for co-expressed hERG1a/1b (smaller than for hERG1a alone under identical conditions [12]), consistent with enhanced heterogeneity in repolarizing I_{Kr} between ventricular and PF APs in SQT1.

To-date there is comparatively little information available on the effects of clinically relevant hERG mutations on hERG1a/1b heteromers [16]. This is the first study to have investigated hERG1a/1b heteromeric channels in the context of the short QT syndrome and it is only the second that provides detailed information on biophysical properties of WT $I_{hERG1a/1b}$, at a physiologically relevant temperature. Our findings support the notion that the contribution to ventricular repolarization of current through heteromeric WT hERG1a/1b channels differs from that of hERG1a alone [16]. More remarkably, they demonstrate for the first time a marked difference in the inactivation-attenuating effect of a pathologically relevant hERG mutation when heteromeric hERG1a/1b channels are studied. N-terminal deletion has been demonstrated to slow hERG1a inactivation [25] and the amplified effect of the N588K mutation on fractional inactivation of $I_{hERG1a/1b}$ seen here may reflect synergy between the mutation's disruption of the role of the S5-Pore linker in the inactivation process and the potential for reduced stabilization of inactivation due to the fact that 1a/1b heteromers have fewer N-terminal contacts to interact with the internal S4–S5 linker [16,25]. Whilst it may be intuitively obvious that the study of hERG1b-specific mutations [16] or N-terminal long QT syndrome (LQTS) mutations (∼20% of

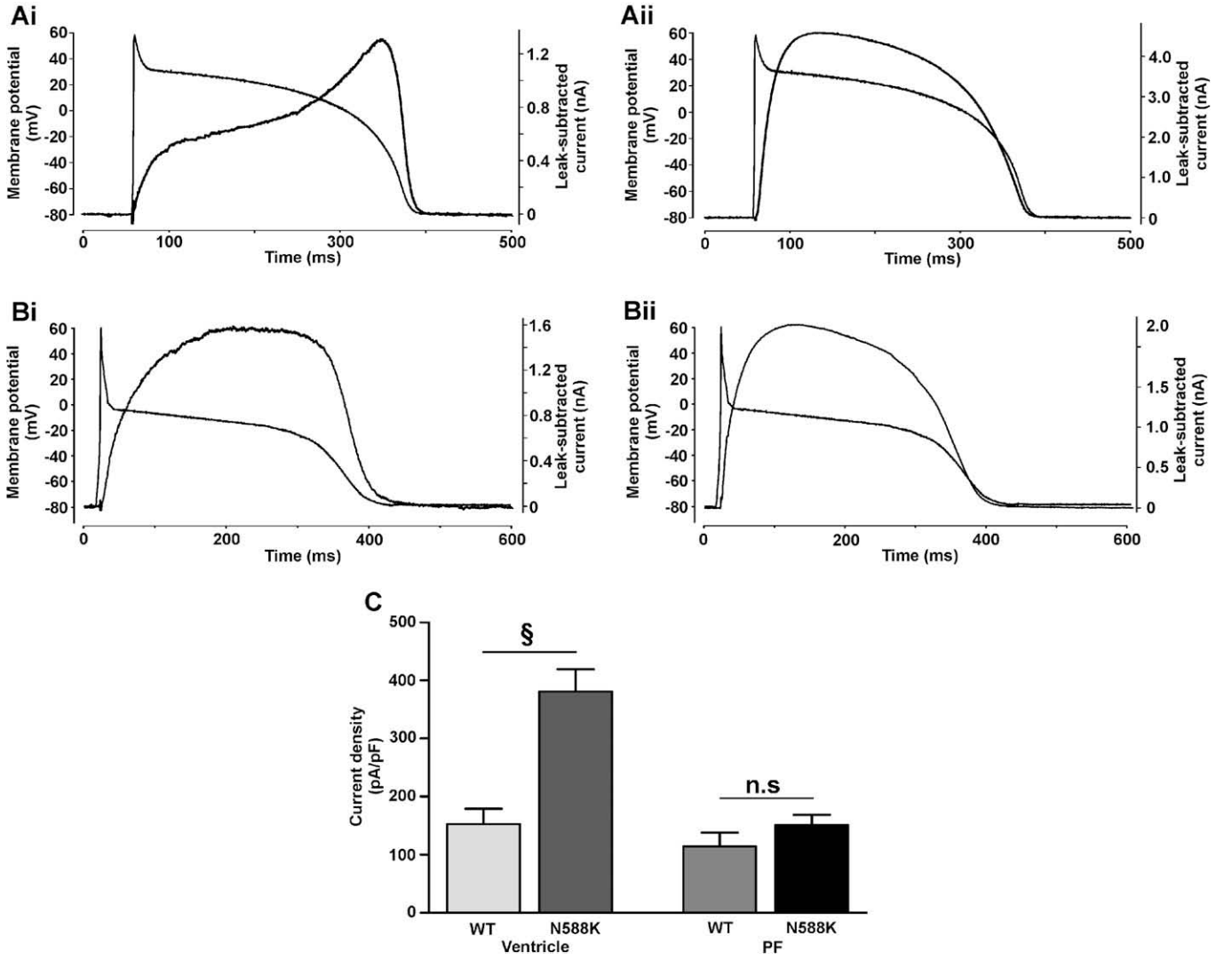

Fig. 4. $I_{hERG1a/1b}$ profile during ventricular and Purkinje fibre AP waveforms. (A) Representative traces of WT (Ai) and N588K (Aii) $I_{hERG1a/1b}$ elicited by ventricular AP command waveform (shown overlain; $n = 14$ for both). (B) Representative traces of WT (Bi; $n = 13$) and N588K (Bii; $n = 14$) $I_{hERG1a/1b}$ elicited by a Purkinje fibre AP command waveform. (C) Plots of maximal current density for WT and N588K hERG1a/1b during ventricular and Purkinje fibre AP command waveforms. § denotes statistical significance of $P < 0.001$.

hERG1a-linked LQTS mutations occur in the N-terminus [26]) warrants the study of hERG1a/1b heteromeric channels, until now there may not have been a clear rationale to adopt this approach when studying mutations that are distant from the N-terminus. The present study provides a clear demonstration that such mutations cannot be assumed to have identical effects on hERG1a/1b to those found for hERG1a alone. Consequently, it may be prudent to incorporate more widely the study of hERG1a/1b heteromeric channels when investigating biophysical consequences of hERG mutations in both the LQTS and SQTS.

Acknowledgment

This study was funded by the British Heart Foundation (PG/06/139).

References

[1] I. Gussak, P. Brugada, J. Brugada, R.S. Wright, S.I. Kopecky, B.R. Chaitman, P. Bjeerregaard, Idiopathic short QT interval: a new clinical syndrome?, Cardiology 94 (2000) 99–102

[2] F. Gaita, C. Giustetto, F. Bianchi, C. Wolpert, R. Schimpf, R. Riccardi, S. Grossi, E. Richiardi, M. Borggrefe, Short QT syndrome: a familial cause of sudden death, Circulation 108 (2003) 965–970.

[3] R. Schimpf, C. Wolpert, F. Gaita, C. Giustetto, M. Borggrefe, Short QT syndrome, Cardiovasc. Res. 67 (2005) 357–366.

[4] P. Maury, F. Extramiana, P. Sbragia, C. Giustetto, R. Schimpf, A. Duparc, C. Wolpert, I. Denjoy, M. Delay, M. Borggrefe, F. Gaita, Short QT syndrome. Update on a recent entity, Arch. Cardiovasc. Dis. 101 (2008) 779–786.

[5] R. Brugada, K. Hong, R. Dumaine, J. Cordeiro, F. Gaita, M. Borggrefe, T.M. Menendez, J. Brugada, G.D. Pollevick, C. Wolpert, E. Burashnikov, K. Matsuo, Y.S. Wu, A. Guerchicoff, F. Bianchi, C. Giustetto, R. Schimpf, P. Brugada, C. Antzelevitch, Sudden death associated with short-QT syndrome linked to mutations in HERG, Circulation 109 (2004) 30–35.

[6] K. Hong, P. Bjeerregaard, I. Gussak, R. Brugada, Short QT syndrome and atrial fibrillation caused by mutation in *KCNH2*, J. Cardivasc. Electophysiol. 16 (2005) 394–396.

[7] C. Bellocq, A.C. van Ginneken, C.R. Bezzina, M. Alders, D. Escande, M.M. Mannens, I. Baro, A.A. Wilde, Mutation in the *KCNQ1* gene leading to the short QT-interval syndrome, Circulation 109 (2004) 2394–2397.

[8] C. Giustetto, M.F. Di, C. Wolpert, M. Borggrefe, R. Schimpf, P. Sbragia, G. Leone, P. Maury, O. Anttonen, M. Haissaguerre, F. Gaita, Short QT syndrome: clinical findings and diagnostic-therapeutic implications, Eur. Heart J. 27 (2006) 2440–2447.

[9] M. Cerrone, S. Noujaim, J. Jalife, The short QT syndrome as a paradigm to understand the role of potassium channels in ventricular fibrillation, J. Int. Med. 259 (2006) 24–38.

[10] J.S. Mitcheson, M.C. Sanguinetti, Biophysical properties and molecular basis of cardiac rapid and slow delayed rectifier K channels, Cell. Physiol. Biochem. 9 (1999) 201–216.
[11] J.M. Cordeiro, R. Brugada, Y.S. Wu, K. Hong, R. Dumaine, Modulation of I_{Kr} inactivation by mutation N588K in *KCNH2*: a link to arrhythmogenesis in short QT syndrome, Cardiovasc. Res. 67 (2005) 498–509.
[12] M.J. McPate, R.S. Duncan, J.T. Milnes, H.J. Witchel, J.C. Hancox, The N588K-HERG K^+ channel mutation in the 'short QT syndrome': mechanism of gain-in-function determined at 37 °C, Biochem. Biophys. Res. Commun. 334 (2005) 441–449.
[13] M.J. McPate, H. Zhang, I. Ideniran, J.M. Cordeiro, H.J. Witchel, J.C. Hancox, Comparative effects of the short QT N588K mutation at 37 °C on hERG K^+ channel current during ventricular, Purkinje fibre and atrial action potentials: an action potential clamp study, J. Physiol. Pharmacol. 60 (2009) 23–41.
[14] M. Grunnet, T.G. Diness, R.S. Hansen, S.P. Olesen, Biophysical characterization of the short QT mutation hERG-N588K reveals a mixed gain-and loss-of-function, Cell. Physiol. Biochem. 22 (2008) 611–624.
[15] E.M. Jones, E.C. Roti Roti, J. Wang, G.A. Robertson, Cardiac I_{Kr} channels minimally comprise hERG 1a and 1b subunits, J. Biol. Chem. 279 (2004) 44690–44694.
[16] H. Sale, J. Wang, T.J. O'Hara, D.J. Tester, P. Phartiyal, J.Q. He, Y. Rudy, M.J. Ackerman, G.A. Robertson, Physiological properties of hERG 1a/1b heteromeric currents and a hERG 1b-specific mutation associated with long-QT syndrome, Circ. Res. 103 (2008) e81–e95.
[17] J.P. Lees-Miller, C. Kondo, L. Wang, H.J. Duff, Electrophysiological characterization of an alternatively processed ERG K^+ channel in mouse and human hearts, Circ. Res. 81 (1997) 719–726.
[18] B. London, M.C. Trudeau, K.P. Newton, A.K. Bayer, N.G. Copeland, D.J. Gilbert, N.A. Jenkins, C.A. Satler, G.A. Robertson, Two isoforms of the mouse ether-a-go-go related gene coassemble form channels with properties similar to the rapidly activating component of the cardiac delayed rectifier K current, Circ. Res. 81 (1997) 870–878.
[19] A.L. Pond, B.K. Scheve, A.T. Benedict, K. Petrecca, D.R. van Wagoner, A. Shrier, J.M. Nerbonne, Expression of distinct ERG proteins in rat, mouse, and human heart. Relation to functional I_{Kr} channels, J. Biol. Chem. 275 (2000) 5997–6006.
[20] A.P. Larsen, S.P. Olesen, M. Grunnet, T. Jespersen, Characterization of hERG1a and hERG1b potassium channels – a possible role for hERG1b in the I_{Kr} current, Pflugers Arch. 456 (2008) 1137–1148.
[21] J.T. Milnes, O. Crociani, A. Arcangeli, J.C. Hancox, H.J. Witchel, Blockade of HERG potassium currents by fluvoxamine: incomplete attenuation by S6 mutations at F656 or Y652, Br. J. Pharmacol. 139 (2003) 887–898.
[22] M.J. McPate, R.S. Duncan, J.C. Hancox, H.J. Witchel, Pharmacology of the short QT syndrome N588K-hERG K^+ channel mutation: differential impact on selected class I and class III antiarrhythmic drugs, Br. J. Pharmacol. 155 (2008) 957–966.
[23] M.J. McPate, R.S. Duncan, H.J. Witchel, J.C. Hancox, Disopyramide is an effective inhibitor of mutant HERG K^+ channels involved in variant 1 short QT syndrome, J. Mol. Cell. Cardiol. 41 (2006) 563–566.
[24] J.C. Hancox, A.J. Levi, H.J. Witchel, Time course and voltage dependence of expressed HERG current compared with native 'rapid' delayed rectifier K current during the cardiac ventricular action potential, Pflugers Arch. Eur. J. Physiol. 436 (1998) 843–853.
[25] J. Wang, M.C. Trudeau, A.M. Zappia, G.A. Robertson, Regulation of deactivation by an amino terminal domain in HERG potassium channels, J. Gen. Physiol. 112 (1998) 637–647.
[26] G.A. Robertson, E.M. Jones, J. Wang, Gating and assembly of heteromeric hERG1a/1b channels underlying I_{Kr} in the heart Novartis, Found. Symp. 266 (2005) 4–15.